Boundary-Layer Meteorology (2006) 118: 217–240
DOI 10.1007/s10546-005-4736-1

BUOYANCY AND THE SENSIBLE HEAT FLUX BUDGET WITHIN DENSE CANOPIES

D. CAVA[1,*], G. G. KATUL[2], A. SCRIMIERI[1,3], D. POGGI[2,4,5], A. CESCATTI[6] and U. GIOSTRA[7]

[1]*CNR – Institute of Atmosphere Sciences and Climate section of Lecce, Lecce, Italy;* [2]*Nicholas School of the Environment and Earth Sciences,Duke University, Durham, North Carolina, U.S.A.;* [3]*Department of Material Science, University of Lecce, Lecce, Italy;* [4]*Department of Civil and Environmental Engineering, Duke University, Durham, North Carolina, U.S.A.;* [5]*Dipartimento di Idraulica, Trasporti ed Infrastrutture Civili, Politecnico di Torino, Torino, Italy;* [6]*Centro di Ecologia Alpina, 38040 Viote del Monte Bondone (Trento), Italy;* [7]*Department of Environmental Science, University of Urbino, Urbino, Italy*

(Received in final form 23 February 2005)

Abstract. In contrast to atmospheric surface-layer (ASL) turbulence, a linear relationship between turbulent heat fluxes (F_T) and vertical gradients of mean air temperature within canopies is frustrated by numerous factors, including local variation in heat sources and sinks and large-scale eddy motion whose signature is often linked with the ejection-sweep cycle. Furthermore, how atmospheric stability modifies such a relationship remains poorly understood, especially in stable canopy flows. To date, no explicit model exists for relating F_T to the mean air temperature gradient, buoyancy, and the statistical properties of the ejection-sweep cycle within the canopy volume. Using third-order cumulant expansion methods (CEM) and the heat flux budget equation, a "diagnostic" analytical relationship that links ejections and sweeps and the sensible heat flux for a wide range of atmospheric stability classes is derived. Closure model assumptions that relate scalar dissipation rates with sensible heat flux, and the validity of CEM in linking ejections and sweeps with the triple scalar-velocity correlations, were tested for a mixed hardwood forest in Lavarone, Italy. We showed that when the heat sources (S_T) and F_T have the same sign (i.e. the canopy is heating and sensible heat flux is positive), sweeps dominate the sensible heat flux. Conversely, if S_T and F_T are opposite in sign, standard gradient-diffusion closure model predict that ejections must dominate the sensible heat flux.

Keywords: Buoyancy, Canopy turbulence, Cumulant expansions, Ejections and sweeps, Heat flux budget, Nonlocal transport, Organized eddy motion, Second-order closure models.

1. Introduction

Over the past two decades, substantial progress was made in studying large-scale organized eddy motion and in linking them to countergradient (or zero-gradient) flows within canopies (Wilson and Shaw, 1977; Finnigan,

*E-mail: d.cava@isac.cnr.it

1979; Raupach, 1981, 1989a, b; Gao et al., 1989; Shaw et al., 1989; Wilson, 1989; Leclerc et al., 1990, 1991; Kaimal and Finnigan, 1994; Finnigan, 2000). Unequivocal experimental evidence for the failure of the so-called K theory (or gradient-diffusion theory) in canopies came about from detailed scalar concentration and flux profile measurements within the Uriarra forest in Australia by Denmead and Bradley (1985). These measurements revealed that co-gradient flow of heat, water vapour, and CO_2 do exist near the canopy top but zero or countergradient flow can exist in the mid to lower canopy levels. Later studies (e.g. see the review in Thurtell, 1989; Wilson, 1989; Kaimal and Finnigan, 1994) also revealed that zero or countergradient flows primarily occur because (1) the variable scalar source distribution (S) within the canopy strongly affects the apparent diffusivity (i.e. the ratio of the local flux to the local gradient), as discussed in Raupach (1983, 1987, 1989a, b), Raupach et al. (1986) and Wilson (1989); (2) much of the vertical transport is influenced by eddy motion whose scale is comparable to the canopy height (h_c) rather than height from the ground surface (z) (e.g. Corrsin, 1974; Finnigan, 1979; Wilson, 1989); and (3) canopy turbulence lacks any local equilibrium (i.e. a region in which local production of turbulent kinetic energy (TKE) is balanced by local viscous dissipation) as discussed in Shaw (1977) and later by Maitani and Seo (1985). The lack of local equilibrium often necessitates the use of higher-order closure models for linking fluxes to gradients.

While this emerging picture appeals to near-neutral canopy flows, much less is known about the role of thermal stratification in modifying the relationship between scalar fluxes and mean gradients, especially for mildly stable and stable canopy flows (Mahrt, 1998). How the interplay between ejections and sweeps, often used as signatures of large-scale organized motion, and local thermal stability affects the onset of zero or countergradient flows remains an active research subject with broad implications for numerous practical problems, such as developing and testing higher-order closure models for canopy scalar transport, or inferring S from mean scalar concentration profiles (e.g., see Raupach, 1989a, b; Katul et al., 1997a; Katul and Albertson, 1999; Leuning et al., 2000; Siqueira et al., 2002, 2003). What is clearly lacking is an analytical framework that diagnoses the onset of zero and countergradient flows based on the relative importance of ejections and sweeps (i.e. effects of organized eddy motion) and for a wide range of atmospheric stability conditions. Also, such a framework can offer rich diagnostic tools for testing higher-order closure principles within canopies in ways not previously attempted.

Here, a simplified analytical "diagnostic" model that connects the local density gradients and the relative importance of ejections and sweeps to the flux-gradient relationship of air temperature (T) within canopies for unstable, mildly stable, and stable flows is derived. Our choice of T as a

"reference" scalar is attributed to the fact that temperature is not passive since it affects the TKE budget; hence, atmospheric stability is likely to have more impact on temperature fluctuations when compared to other scalars (e.g. Katul and Parlange, 1994). The analytical model derived here makes use of two principles: (1) the turbulent flux budget equation modified to account for thermally stratified flows (e.g. Meyers and Paw U, 1987; Wilson, 1989; Siqueira et al., 2002), (2) an incomplete cumulant expansion formulation proposed by Katul et al. (1997b) and tested by Poggi et al. (2004) that links the flux transport term to the ejection-sweep cycle. The coupling between the momentum flux transport term and the ejection-sweep cycle was successfully established using cumulant expansion methods (CEM) in open channel and wind-tunnel boundary-layer flows (e.g. Nakagawa and Nezu, 1977; Raupach, 1981) though its application to scalar transport inside canopies received much less attention. The connection between the "bursting" phenomena and heat transport via CEM in open channel flows has already been formulated by Nagano and Tagawa (1995) and their success serves as a logical starting point to the study objectives here.

The main theoretical novelty is the analytical linkage between gradient-diffusion closure schemes applied to the turbulent flux transport term of the heat flux budget equation via CEM and the ejection-sweep eddy motion. These linkages are established using two inter-related formulations – the first being a *prognostic* formulation (e.g. gradient-diffusion closure for higher-order terms) that predicts sensible heat fluxes from measured mean temperature gradients, while the second is a *diagnostic* formulation that shows how the relative importance of ejections and sweeps can modify the relationship between sensible heat and mean temperature gradients.

We show that second-order closure models employing gradient-diffusion closure for the triple velocity temperature correlation can reproduce the relative importance of ejections and sweeps within the canopy for unstable and stable flows despite local closure approximations. The assumptions used in the proposed approach are independently verified using detailed multilevel heat flux experiments conducted within a mixed hardwood forest in Lavarone, Italy, described next.

2. Experimental Facilities

While much of the experimental set-up is already presented in Marcolla et al. (2003), a brief review is provided for completeness. The site is an uneven-aged mixed coniferous forest on an alpine plateau (Lavarone, Italian Alps; 45.96° N, 11.28° E; 1300 m asl). This site is part of a long-term CO_2 flux monitoring initiative known as CarboEuroflux (Valentini et al.,

2000). The canopy is primarily composed of *Abies alba* (70%), *Fagus sylvatica* (15%), and *Picea abies* (15%). The mean canopy height (h_c) is about 28–30 m and the lower limit of tree crowns is at about 10–12 m. The maximum leaf area index (LAI) is 9.6, expressed as half of the total leaf area per unit ground area (Chen and Black, 1992). The observations analysed here were collected as part of a summertime intensive measurement campaign performed in 2000 (Julian Days 222–251).

The turbulent statistics and mean temperature gradients were collected at a micrometeorological tower situated on a gently rolling plateau and surrounded by homogeneous vegetation for radial distances exceeding 1 km (except for a 45° section in the south and south-west directions for which vegetation uniformity is only 300 m). The tower was equipped with five flux instruments situated at 33, 25, 17.5, 11 and 4 m from the forest floor. The flux instrument at the tower top (= 33 m) is about 3–5 m above the canopy, the lowest (= 4 m) is in the trunk space, while the intermediate three anemometers (25, 17.5, and 11 m) are at the top, in the middle and at the bottom of the crown layer, respectively. The turbulent wind velocity components and sonic anemometry temperature were sampled at 20 Hz for the highest and the lowest levels by a Gill R3 ultrasonic anemometers (Gill Instrument, Lymington, U.K.). At the remaining levels, only turbulent wind velocity components and sonic anemometer temperature were each sampled by Gill R2 ultrasonic anemometers (Gill Instrument, Lymington, U.K.) at 20.8 Hz. Finally, the half-hourly averaged temperature was sampled by thermocouple sensors at seven measurement heights (28, 24, 20, 16, 12, 8 and 4 m). Half-hourly mean values of the main turbulence statistics were computed for each level following two coordinate rotations to ensure the mean lateral and vertical velocities were zero. Data were grouped according to three atmospheric stability classes using the measured h_c/L (where L is the Obukhov length measured at the canopy top). These classes are labelled as *class A* for unstable atmospheric conditions ($h_c/L < 0$); *class B* for near neutral or weakly stable atmospheric conditions ($0 < h_c/L < 0.5$); and *class C* for strongly stable conditions ($h_c/L > 0.5$).

Before computing the "ensemble" statistics for each stability class, runs exhibiting clear nonstationarity were discarded. Overall, the experiment resulted in 50 runs for class A, 46 runs for class B, and 41 runs for class C. These data were used to test assumptions employed in the model development.

3. Theory

To address the study objective, a model that links sensible heat flux, mean air temperature gradient, atmospheric stability, and the ejection-sweep cycle

(a signature of large-scale eddy motion) is developed here. Our starting point is the time and horizontally averaged sensible heat flux ($=\langle\overline{w'T'}\rangle$) budget equation, described next.

3.1. Heat flux budget model

For a planar homogeneous, stationary, high Reynolds number, and high Peclet number flow (neglecting molecular diffusion), the heat flux budget reduces to (Wilson, 1989):

$$\frac{\partial\langle\overline{w'T'}\rangle}{\partial t}=0=-\langle\overline{w'^2}\rangle\frac{\partial\langle\overline{T}\rangle}{\partial z}-\frac{\partial\langle\overline{w'w'T'}\rangle}{\partial z}-\frac{1}{\rho}\left\langle\overline{T'\frac{\partial p'}{\partial z}}\right\rangle+\frac{g}{\langle\overline{T}\rangle}\langle\overline{T'^2}\rangle. \qquad (1)$$

The overbar and $\langle\cdot\rangle$ indicate, respectively, time and horizontal averaging (Raupach and Shaw, 1982); a prime denotes a fluctuation from the time average; w is the vertical velocity, p is the pressure and ρ is the mean air density. We use both σ_c^2 and $\langle\overline{c'c'}\rangle$ to indicate the variance of any turbulent flow variable c'. The terms on the right-hand side of Equation (1) represent, respectively, the production of turbulent heat flux due to the interaction between turbulence and the mean air temperature gradient (PR), the heat transport by turbulent motion (TR), the decorrelation due to the pressure–temperature interaction (D), and the buoyant production or destruction (B). For simplicity, we neglected the effect of water vapour concentration fluctuations on B. The terms PR, TR, and B can be estimated at a single tower from standard instrumentation (e.g. see Section 2). On the other hand, the D is unknown, difficult to measure, and requires closure approximations. Finnigan (1985) used the following model for D, originally proposed by Wyngaard (1982) for boundary-layer turbulence:

$$\frac{1}{\rho}\left\langle\overline{T'\frac{\partial p'}{\partial z}}\right\rangle=C_4\frac{\langle\overline{w'T'}\rangle}{\tau}-\frac{1}{3}\frac{g}{\langle\overline{T}\rangle}\langle\overline{T'^2}\rangle. \qquad (2)$$

In Equation (2), C_4 is a closure constant (2.5–3.0) and τ is a Eulerian relaxation time scale. Within the literature, two (inconsistent) estimates of τ have been proposed. The first is based on a constant Lagrangian time within the canopy (e.g. Raupach, 1989a, b), along with a proportional relationship between this Lagrangian time scale and τ derived by relating the Eulerian and Lagrangian spectra within the inertial subrange. The second assumes that the mixing length scale is constant within the canopy, which logically leads to a height-dependent τ (Massman and Weil, 1999; Poggi et al., 2004, 2005). Detailed laser-doppler anemometery measurements of TKE and its dissipation within a dense canopy in a flume suggested that τ is best approximated from a constant mixing length scale argument, which leads to (Poggi et al., 2005):

$$\tau = \begin{cases} \beta \dfrac{h_c}{\sigma_w} & \text{for } z/h_c < 0.75, \quad (3a) \\ \dfrac{k(z-d)u_*}{\sigma_w^2} & \text{for } z/h_c > 0.75, \quad (3b) \end{cases}$$

where $k = 0.4$ is the von Karman constant, d is the zero-plane displacement height ($\approx (2/3)h_c$)) and $\beta = 0.1$ as suggested by Poggi et al. (2005) for dense canopies (as is the case here).

Upon combining Equations (1) and (2), the sensible heat flux can be written as (Wilson, 1989):

$$\langle \overline{w'T'} \rangle = \frac{\tau}{C_4} \left[-\langle \overline{w'^2} \rangle \frac{\partial \langle \overline{T} \rangle}{\partial z} - \frac{\partial \langle \overline{w'w'T'} \rangle}{\partial z} + \frac{4}{3} \frac{g}{\langle \overline{T} \rangle} \langle \overline{T'^2} \rangle \right]. \quad (4)$$

The above equation establishes the well-known conditions for the failure of gradient-diffusion theory in modelling $\overline{w'T'}$. Only when both flux transport and buoyant production terms are negligible, the usual flux-gradient relationship is recovered. We examine next the use of classical second-order closure models for parameterizing $\langle \overline{w'w'T'} \rangle$, and proceed to explicitly show the connections between sensible heat flux, and ejections and sweeps via a new model for $\langle \overline{w'w'T'} \rangle$.

3.2. Triple velocity–temperature correlations and their gradient-diffusion Closure

Consider the simplest gradient-diffusion closure model for $\langle \overline{w'w'T'} \rangle$ given by

$$\langle \overline{w'w'T'} \rangle = -C_5 \tau \sigma_w^2 \frac{d \langle \overline{w'T'} \rangle}{dz}, \quad (5)$$

where C_5 is a closure constant with reported values ranging from 1.5 to 8.0. A value of 1.5 was reported for a rice canopy by Katul et al. (2001), 3.0 reported for a pine canopy by Siqueira and Katul (2002), and 8.0 reported in Meyers and Paw U (1987) based on an optimization conducted by André et al. (1979) for a convective tank experiment. The reason why C_5 appears widely variable across studies is perhaps due to τ estimates not being consistent (especially in how the mean TKE dissipation rate is computed or modelled). The mean air temperature continuity equation can be used to link the heat flux profile to the mean heat source (S_T) using

$$\frac{d \langle \overline{w'T'} \rangle}{dz} = S_T(z), \quad (6)$$

which, when combined with Equations (5) and (4), results in

$$\langle\overline{w'T'}\rangle = \frac{\tau}{C_4}\left[-\langle\overline{w'^2}\rangle\frac{\partial\langle\overline{T}\rangle}{\partial z} + C_5\frac{\partial\tau(z)\sigma_w^2 S_T(z)}{\partial z} + \frac{4}{3}\frac{g}{\langle\overline{T}\rangle}\langle\overline{T'^2}\rangle\right]. \tag{7}$$

Equation (7) is the Eulerian version of the Lagrangian localized near field (LNF) theory put forth by Raupach (1988, 1989a, b) and it explicitly demonstrates how local variations in S_T and atmospheric stability affect the classical flux-gradient relationship (i.e. analogous to the near-field effects in LNF). Equation (7) accounts for the large-scale eddy motion because the canonical length scale of τ is h_c (not z). In short, Equation (7) appears to account for all three arguments stated in the introduction as to why zero and countergradient flows occur. Nevertheless, the connection between the gradient-diffusion closure scheme in Equation (5) and the ejection-sweep cycle remains implicit (except through the length scale). Its explicit form is explored next.

3.3. Connecting the ejection-sweep cycle with turbulent flux transport

The flux transport, $\langle\overline{w'w'T'}\rangle$, can be linked to large-scale organized eddy motion following the approach pioneered by Nakagawa and Nezu (1977) for momentum in which $-\partial\langle\overline{w'w'T'}\rangle/\partial z$ varies according to the relative importance of ejections and sweeps. The relative importance of ejections and sweeps on the turbulent heat flux is commonly quantified via quadrant analysis. Quadrant analysis refers to the joint scatter of two turbulent quantities (e.g. u' and w' for momentum flux, or T' and w' for heat flux) and is used to assess which two quadrants primarily contribute to the turbulent flux. By defining the four quadrants by the Cartesian axes (abscissa u' or T' and ordinate w') events in quadrants 2 and 4 define, respectively, ejections and sweeps for momentum flux. For scalars (in particular for temperature) ejections and sweeps structures are defined by odd or even quadrants depending on the atmospheric stability: for unstable stratification, ejections and sweeps reside in quadrants 3 and 1, while for stable stratification they reside in quadrants 2 and 4, respectively.

One popular measure of the relative importance of ejections and sweeps is the difference in the stress function, defined as (Raupach, 1981):

$$\Delta S_o = \frac{\langle\overline{c'w'}\rangle|_{\text{sweeps}} - \langle\overline{c'w'}\rangle|_{\text{ejections}}}{\langle\overline{c'w'}\rangle}, \tag{8}$$

where c' may be u' or T' for momentum flux or heat flux, respectively. Moreover, the indices defining ejections and sweeps can change with atmospheric stability. To connect these definitions to Equation (1), we follow

Nakagawa and Nezu (1977) and Raupach (1981) who proposed a third-order CEM to link ΔS_o with TR (for quadrants 2 and 4). In particular, Raupach (1981) showed that

$$\Delta S_o = \frac{R_{cw}+1}{R_{cw}\sqrt{2\pi}}\left[\frac{2C_1}{(1+R_{cw})^2}+\frac{C_2}{1+R_{cw}}\right] \tag{9}$$

reproduces measured ΔS_o for momentum reasonably well in a wind-tunnel boundary-layer flow, where

$$R_{cw} = \frac{\langle\overline{c'w'}\rangle}{\sigma_c\sigma_w}$$

is the correlation coefficient; moreover:

$$C_1 = (1+R_{cw})\left[\frac{1}{6}(M_{03}-M_{30})+\frac{1}{2}(M_{21}-M_{12})\right],$$
$$C_2 = -\left[\frac{1}{6}(2-R_{cw})(M_{03}-M_{30})+\frac{1}{2}(M_{21}-M_{12})\right],$$

and

$$M_{ji} = \frac{\langle\overline{c'^j w'^i}\rangle}{\sigma_c^j \sigma_w^i}, \quad \sigma_s = \sqrt{\langle s'^2\rangle}.$$

Katul et al. (1997b) obtained a further simplification to Equation (9) by demonstrating that the mixed moments M_{12} and M_{21} contribute to ΔS_o much more than the combination of M_{03} and M_{30} leading to

$$\Delta S_o \approx \frac{1}{2R_{cw}\sqrt{2\pi}}\left[(M_{21}-M_{12})\right]. \tag{10}$$

We refer to the expansion in Equation (10) as an incomplete CEM or ICEM. Again, the above derivation holds for quadrants 2 and 4 (or when $R_{wc}<0$); to use this result for quadrants 1 and 3 (or when $R_{wc}>0$), an axis transformation can be employed. This axis transformation amounts to reversing the sign of T' that leads to M_{12} and R_{wT} also reversing signs. Moreover, Katul et al. (1997b) reported a proportionality between the measured mixed moments at the canopy top, with $M_{21} = \pm|C|\times M_{12}$ (where the sign is positive when $R_{wc}>0$ and it is negative when $R_{wc}<0$). Hence, with these revisions, the model reduces to

$$\Delta S_o \approx \frac{1}{R_{cw}2\sqrt{2\pi}}\left[\gamma\, M_{12}\right], \tag{11}$$

where $\gamma = -(1+|C|)$ and with all other variables computed in the original (or untransformed) axes. In Section 4, we discuss the validity of

CEM and the approximation leading to Equation (11) for a wide range of atmospheric stability conditions. With this approximation, we obtain the following relationship for the triple moment $\langle\overline{w'w'T'}\rangle$:

$$\langle\overline{w'w'T'}\rangle = \frac{2\sqrt{2\pi}\,\Delta S_o\langle\overline{w'T'}\rangle}{\gamma}\sigma_w. \tag{12}$$

This is an alternative parametrization for the triple moment $\langle\overline{w'w'T'}\rangle$ that explicitly reveals the role of ejections and sweeps in the heat flux budget equation though it serves no predictive (or prognostic) purpose. That is, Equation (12) cannot be used for any prognostic calculations of F_T because the profile of ΔS_o is unknown. Nevertheless, it serves as a diagnostic equation both to assess the failure of the mean gradient-diffusion model and to elucidate the role of large-scale organized motion on the sensible heat flux budget equation via their ejection-sweep signature. Upon combining Equations (4) and (12) we obtain a first-order ordinary differential equation (ODE) given by

$$A_1(z)\frac{\partial\langle\overline{w'T'}\rangle}{\partial z} + A_2(z)\langle\overline{w'T'}\rangle = A_3(z), \tag{13}$$

where

$$A_1(z) = \frac{\Delta S_o 2\sqrt{2\pi}\sigma_w}{\gamma},$$
$$A_2(z) = \frac{C_4}{\tau} + \frac{\partial A_1(z)}{\partial z},$$
$$A_3(z) = -\sigma_w\frac{\partial\langle\overline{T}\rangle}{\partial z} + \frac{4}{3}\frac{g}{\langle\overline{T}\rangle}\sigma_T^2.$$

Using the integrating factor method, the general solution of this ODE is:

$$\langle\overline{w'T'(z)}\rangle = \frac{\int_0^z Q(z)e^{\int_0^z P(z)dz}dz + C_I}{e^{\int_0^z P(z)dz}}, \tag{14}$$

where $P(z) = \frac{A_2(z)}{A_1(z)}$ and $Q(z) = \frac{A_3(z)}{A_1(z)}$, and C_I is an integration constant that depends on the boundary condition (i.e. the flux at the forest floor or the canopy top). The solution in Equation (14) addresses the study objectives as it explicitly relates $\langle\overline{w'T'}\rangle$ to $\langle d\overline{T}/dz\rangle$, z, velocity statistics through σ_w^2, ejections and sweeps through ΔS_o, and atmospheric stability through σ_T^2.

Equation (14) also highlights several important attributes about the role of ejections and sweeps on scalar transport for vertically homogeneous flows. For a constant but nonzero P and Q, and for a zero sensible heat flux at the ground surface, the solution reduces to:

$$\langle\overline{w'T'(z)}\rangle = \frac{Q}{P}(1 - e^{(-Pz)}), \tag{15}$$

where $P = C_4\gamma/(2\sqrt{2\pi}\tau\sigma_w\Delta S_o)$. With $\gamma < 0$ and $z \longrightarrow \infty$, $\langle\overline{w'T'}\rangle$ becomes unbounded if $\Delta S_o > 0$ or when sweeps dominate (i.e. physically impossible), and approaches a constant value ($= Q/P$) if $\Delta S_o < 0$ or ejections dominate (i.e. physically realizable). Hence, with height independent σ_w, τ, and ΔS_o, ejections only appear to yield "realizable" solutions to the analytical solution. This finding appears consistent with momentum transport observations for rough-wall boundary layers where σ_w is nearly constant. When the production of TKE is not entirely balanced by its dissipation (i.e. the flux transport term is finite) in the atmospheric surface layer (ASL), it is well documented that ejections dominate momentum transport (Poggi et al., 2004). Given that, for a vertically homogeneous flow, ejections appear to be the preferred mode of heat transport as in Equation (15), it is logical to attribute the existence of sweeps to large vertical inhomogeneity in the flow statistics, particularly ΔS_o and σ_w. Naturally, $P(z)$ and $Q(z)$ are both nonlinear functions of z given that almost all the terms in A_1, A_2, and A_3 vary in a nonlinear manner within the canopy.

Up to this point, we explored two possible formulations for $\langle\overline{w'w'T'}\rangle$, one is prognostic and is based on gradient-diffusion closure, the other is diagnostic and is based on ΔS_o. Hence, linking these two formulations together permits us to further assess what classical closure models predict for ΔS_o, and whether their failure may be connected with its magnitude (and sign). We repeat that the addition of ΔS_o cannot serve any prognostic purpose: simply stated, we are adding to the closure model one more equation (ICEM) and one more unknown ΔS_o. However, the ability of closure models to predict ΔS_o offers new ways to diagnose closure models.

3.4. Connecting the ejection-sweep cycle with the gradient-diffusion closure

If Equation (5) is valid, it must be consistent with Equation (12). Upon replacing Equations (5) and (6) in Equation (11), we obtain the following relationship between ΔS_o and $\langle\overline{w'T'}\rangle$:

$$\Delta S_o = \frac{-\gamma \times C_5}{2\sqrt{2\pi}} \times (\tau\sigma_w) \times \frac{1}{\langle\overline{w'T'}\rangle} S_T. \tag{16}$$

Again, Equation (16) highlights several important relationships between ejections and sweeps, the local heat sources and sinks, and heat fluxes within the canopy not previously explored. According to Equation (16), sweeps dominate the heat flux when $S_T/\langle\overline{w'T'}\rangle > 0$ for unstable flows. Note, $-\gamma$ is positive irrespective of the quadrants being considered. In short, when the ground heat flux is negligible ($\langle\overline{w'T'(0)}\rangle = 0$) and the $S_T(z) > 0$ profile does not change sign, sweeps must dominate the heat flux according to Equation (16) (see Figure 1).

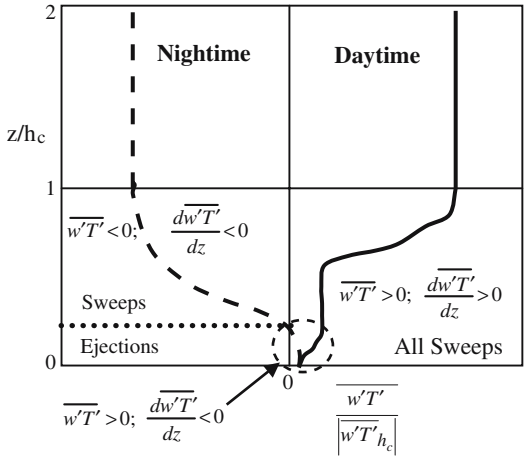

Figure 1. Typical sensible heat flux profiles inside and above the canopy for daytime and nightime conditions, from Kaimal and Finnigan (1994). The flux-gradient closure model for the triple correlation between velocity and temperature *predicts* a positive ΔS_o (i.e. sweeps) throughout the canopy except at nighttime near the forest floor when the flux and its gradient do not share the same sign. These predictions can be compared to measured ΔS_o from quadrant analysis.

Before proceeding, we use the overbar hereafter to indicate both time and spatial averaging for notational simplicity. We also note that from tower-based field experiments, only temporal averages at a point can be measured. The conditions for which the temporal averages, the ensemble averages, and the spatio-temporal averages converge are discussed elsewhere (see Katul et al., 2004).

4. Results

To address the study objectives, we first show that the assumptions and simplifications leading to $\overline{w'T'} = \mathbf{f}(d\overline{T}/dz, z, \sigma_w^2, \Delta S_o, \sigma_T^2)$ are consistent with the measurements here, where **f(.)** is given by Equation (14). In particular, the closure parameterizations in Equation (2), the validity of the ICEM approximation in Equation (10), the linkage between $\overline{w'w'T'}$ and ΔS_o in Equation (12), and the linearity between M_{12} and M_{21} are all explored for the three atmospheric stability classes. The predicted ΔS_o from the second-order closure model is also compared with measured ΔS_o obtained from quadrant analysis for each stability class, a comparison rarely carried out when testing higher-order closure principles for scalar transport. However, before we proceed with these discussions, the effects of atmospheric stability on the heat flux budget components of Equation (1) are explored first to assess their relative magnitudes.

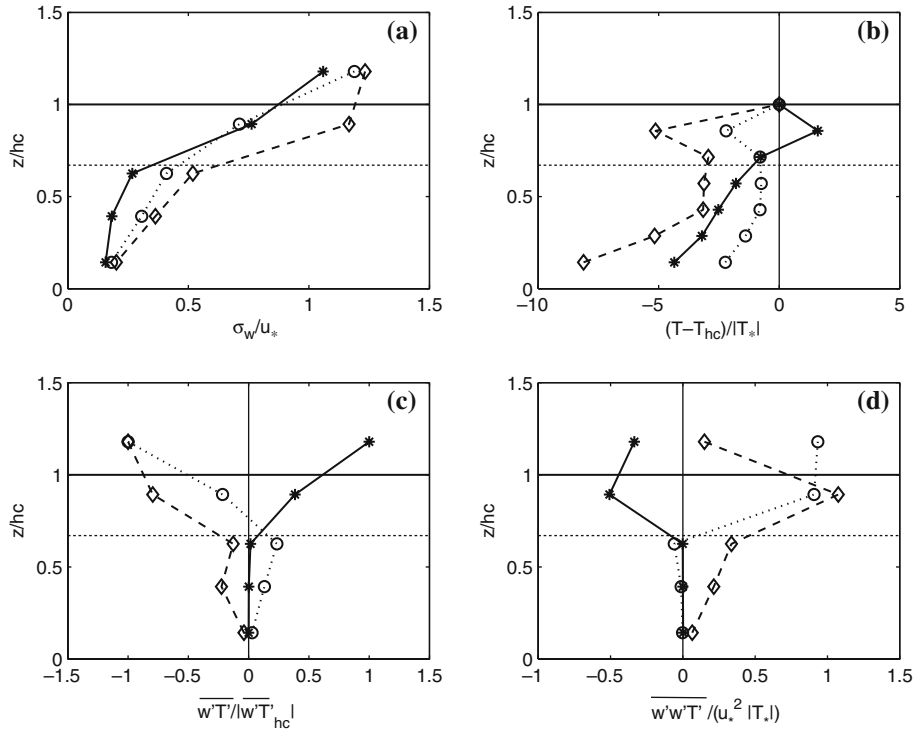

Figure 2. Variation of normalized flow statistics with normalized height (z/h_c) for (a) vertical velocity standard deviation (σ_w/u_*), (b) mean air temperature difference ($\frac{\overline{T}-\overline{T}_{h_c}}{T_*}$), (c) sensible heat flux ($\frac{\overline{w'T'}}{|\overline{w'T'}_{h_c}|}$), and (d) heat flux transport $\frac{\overline{w'w'T'}}{|T_*|{u_*}^2}$, where T_{h_c} is the mean air temperature, $T_* = \frac{\overline{w'T'}_{h_c}}{u_*}$ is a normalizing turbulent temperature scale, and $u_* = (-\overline{u'w'}_{h_c})^{1/2}$ is the friction velocity all defined at the canopy height h_c. The 30-min data runs are ensemble averaged in three stability classes: unstable (∗), weakly stable (◇), and strongly stable (o).

4.1. Stability effects on the heat flux budget components

In Figure 2, the effects of atmospheric stability on the profiles of the vertical velocity variance, mean air temperature, sensible heat flux, and flux transport are shown. These profiles are first presented because they are needed for estimating PR, TR, and B, and they qualitatively illustrate the effects of buoyancy and z on the onset of zero and countergradient flows (see Figure 2b and c) both existing in this forest.

From Figure 2, there is no shortage of examples on zero and countergradient flows within each stability class. Notice how for stable conditions and for $z/h_c \approx 0.3$, a clear countergradient flow exists. Equally noticeable is the zero-gradient flow for stable and slightly stable conditions for $z/h_c \approx 0.6$. Another example is the zero heat flux appearing in the trunk space for unstable stability despite the large mean air temperature gradient and the

significant σ_w/u_*. For the same stability class, a clear countergradient flow also exists around $z/h_c \approx 0.8$.

Using the profiles in Figure 2, we explore the effects of atmospheric stability on the individual components of the sensible heat flux budget equation in Figure 3. Here, PR, TR, and B are either directly measured or independently estimated from the data. Linear interpolation was used to compute gradients of all state variables. The dissipation term D was not measured but was computed as a residual from the budget equation (also shown in Figure 3). Figure 3 suggests that none of these terms can be readily neglected across the entire canopy height irrespective of the stability class. For example, while neglecting B is a common assumption (e.g. Katul and Albertson, 1999; Raupach, 1989a, b), the data here suggest that B can exceed PR at several levels within the canopy even for the near-neutral and mildly stable flows.

Figure 3 also demonstrates that B can be the primary term balancing D within the trunk space of the canopy for stable flows. Hence, Figure 3 confirms that any prognostic or diagnostic relationship between the heat flux and temperature gradient must retain all these terms.

4.2. Testing the dissipation closure model

As discussed in Section 3, given that D cannot be readily measured, it is necessary to link D to "observable" terms. We tested how well the dissipations closure model, proposed by Wyngaard (1982) for boundary-layer turbulence and used by Finnigan (1985) in a similar context, reproduces the ensemble measured $\overline{w'T'}$ within the canopy for all three stability classes, see Figure 4. The vertical variation of the relaxation time scale τ, also needed in this closure model, is shown in Figure 4. The variation of τ remains a subject of debate and clearly is an important source of uncertainty in this closure parameterizations. Nonetheless, the closure model reproduces reasonably well the measured sensible heat flux for a wide range of atmospheric stability conditions when the closure constant C_4 is set to a value of 2.9, a value comparable to C_4 values ($= 2.5 - 3.0$) already reported in Katul et al. (2001) and Siqueira and Katul (2002). Having verified the heat flux dissipation closure model in Figure 4, the next logical step is testing the linkages between ΔS_o and $\overline{w'w'T'}$ via the ICEM.

4.3. Turbulent flux transport, ejections and sweeps, and CEM

In Section 3, third-order CEM was used to link the ejection-sweep cycle with the heat flux transport term in Equation (11). Hence, it is necessary to explore how well third-order CEM and ICEM expansions in Equations (9) and (10) reproduce the measured ΔS_o computed from Equation (8). In

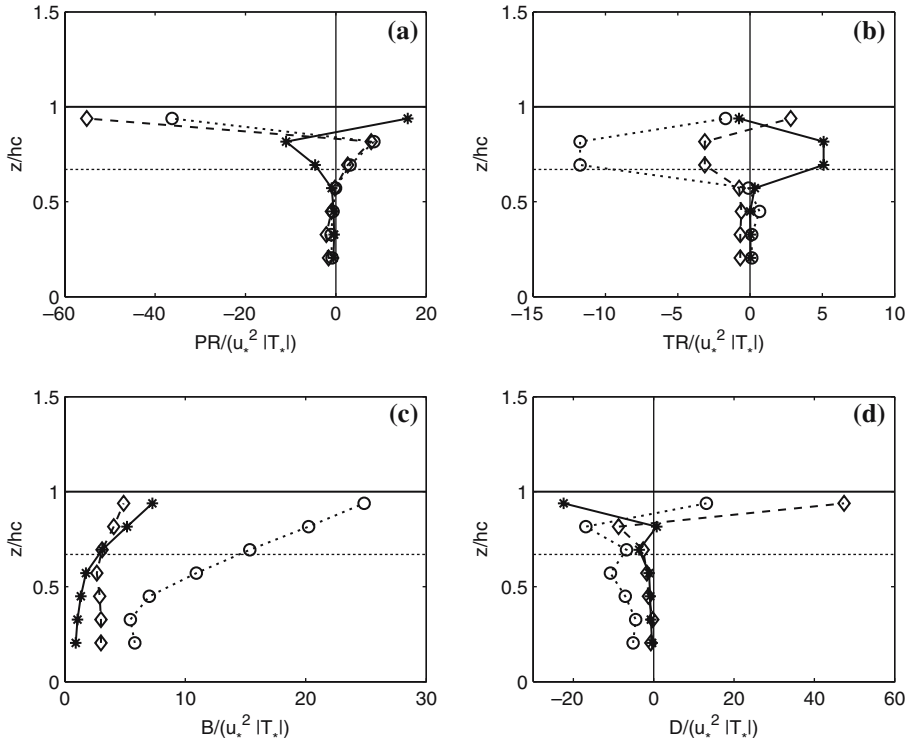

Figure 3. Variation of the normalized components of the sensible heat flux budget equation with normalized height (z/h_c) for (a) the production term ($PR = -\overline{w'w'}\frac{d\overline{T}}{dz}$), (b) the flux transport term $TR = \frac{d\overline{w'w'T'}}{dz}$, (c) the Buoyancy term $B = \frac{g}{\overline{T}}\sigma_T{}^2$, and (d) the scalar dissipation term $D = \overline{T'\frac{dp'}{dz}}$ estimated as a residual from Equation (1). All temperature, velocity, and length scales are normalized by T_*, u_*, and h_c, respectively. The three stability classes are as in Figure 2.

Figures 5 and 6, the comparison between measured and CEM modelled ΔS_o for both momentum and sensible heat fluxes are shown for all three stability cases. It is clear that both CEM and ICEM reproduce the measured ΔS_o profiles reasonably well for both momentum and sensible heat fluxes and for all stability conditions, thereby lending further confidence to third-order ICEM expansions within canopies (Katul et al., 1997b; Poggi et al., 2004). Interestingly, Fer et al. (2004) also demonstrated that the ICEM well reproduces measured ΔS_o in the under-ice boundary layer below drifting pack-ice.

While the ICEM formulation provided the desirable link between $M_{12} = \overline{w'w'T'}/(\sigma_w^2\sigma_T)$ and ΔS_o, it also introduced a new quantity, $M_{21} = \overline{w'T'T'}/(\sigma_w\sigma_T^2)$. Whether M_{21} can be related to M_{12} theoretically remains a challenge, though empirically, few experiments already suggested linearities in

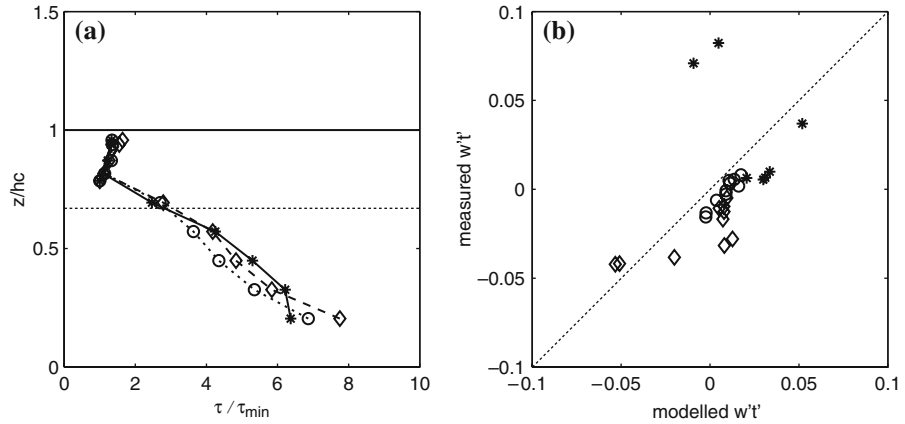

Figure 4. (a) Variation of the normalized time scale (τ) with height (z/h_c); (b) Comparison between measured and modelled $\overline{w'T'}$ for all heights and stability classes. The modelled sensible heat flux is based on modelled (τ) and the dissipation closure scheme in Equation (2). The three stability classes are as in Figure 2. For reference, the 1:1 line is also shown. The linear correlation coefficient of the data is $R = 0.8$.

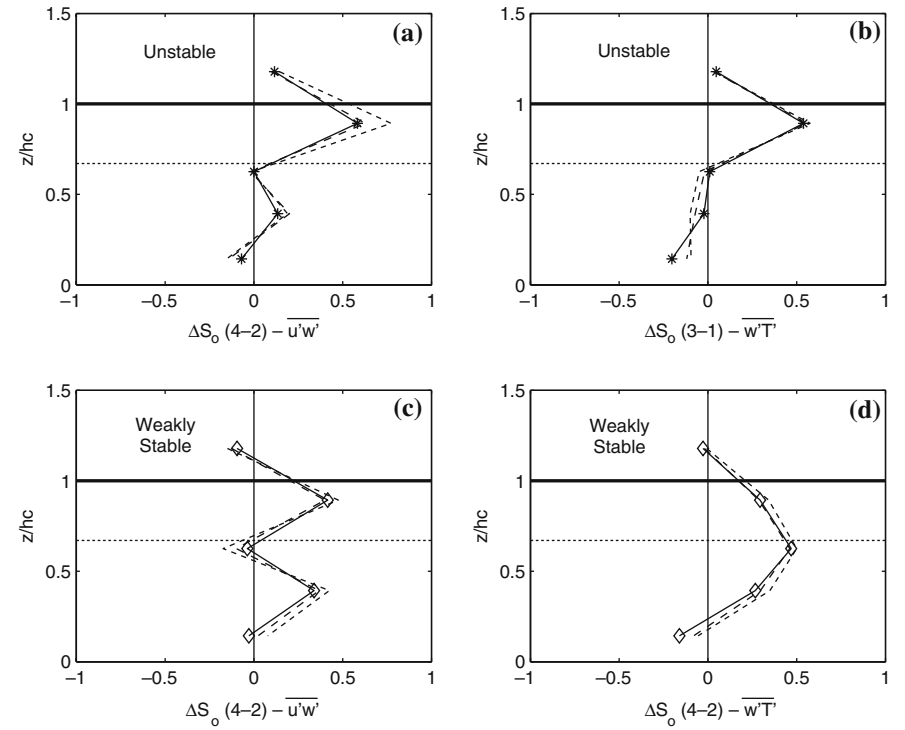

Figure 5. Comparison between measured and modelled ΔS_o for momentum (a, c) and sensible heat (b, d) and for unstable and weakly stable stability classes. The measured ΔS_o is based on Equation (8) and the modelled ΔS_o are based on third-order CEM (dashed) in Equation (9) and the incomplete CEM or ICEM (dot-dashed) in Equation (10). The subscripts (3–1) and (2–4) indicate the quadrants used to compute ΔS_o.

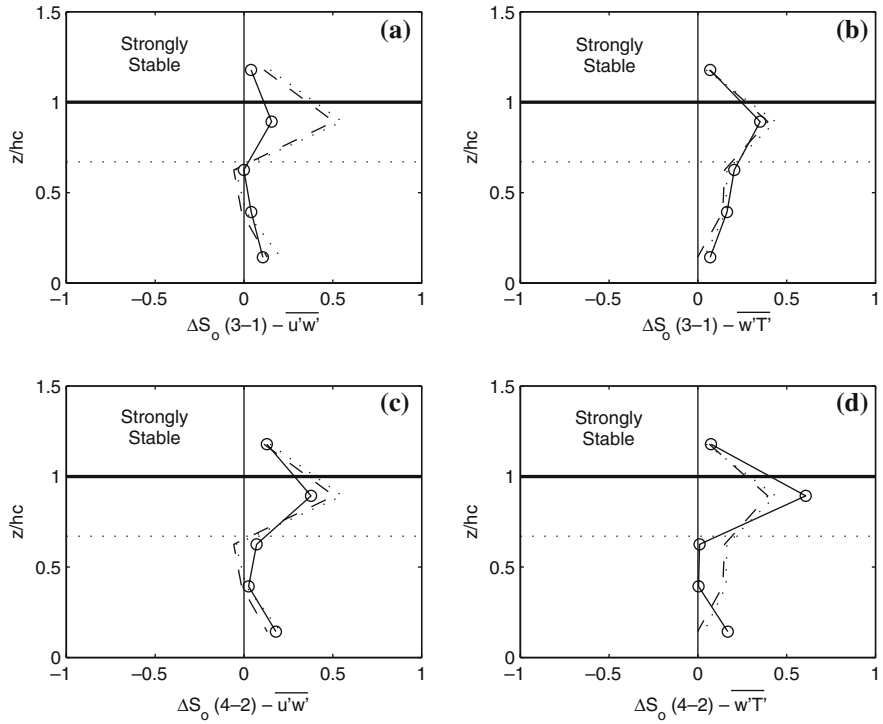

Figure 6. Same as Figure 5 but for strongly stable flows. Given that the sensible heat and momentum fluxes change signs within the canopy, the ΔS_o obtained from quadrants (3, 1) and quadrants (2, 4) are shown for completeness.

momentum (Raupach, 1981) and scalars (Katul et al., 1997b). We tested in Figure 7 whether such a linear relationship also holds for the Lavarone canopy for heat and momentum and for the three stability classes using all the runs. Figure 7 shows that M_{12} is linearly related to M_{21} for unstable, slightly stable, and stable flows consistent with earlier studies on heat and momentum. Interestingly, the value of $|C|(=0.6)$ for both heat and momentum and for all three stability classes is the same as evidenced by Figure 7.

We compared modelled ΔS_o from Equation (16) with measured ΔS_o determined by quadrant analysis in Figure 8 using $C_5 = 2.4$ for all stability classes. Recall that Equation (16) assumes, (1) a linear relationship between M_{12} and M_{21} with a $|C| = 0.6$; (2) a gradient-diffusion closure for $\overline{w'w'T'}$; and (3) a τ determined from a constant mixing length scale (with a $\beta = 0.1$). Despite these simplifications and assumptions, the agreement between measured and modelled ΔS_o is rather encouraging (correlation coefficient $R = 0.65$–0.76).

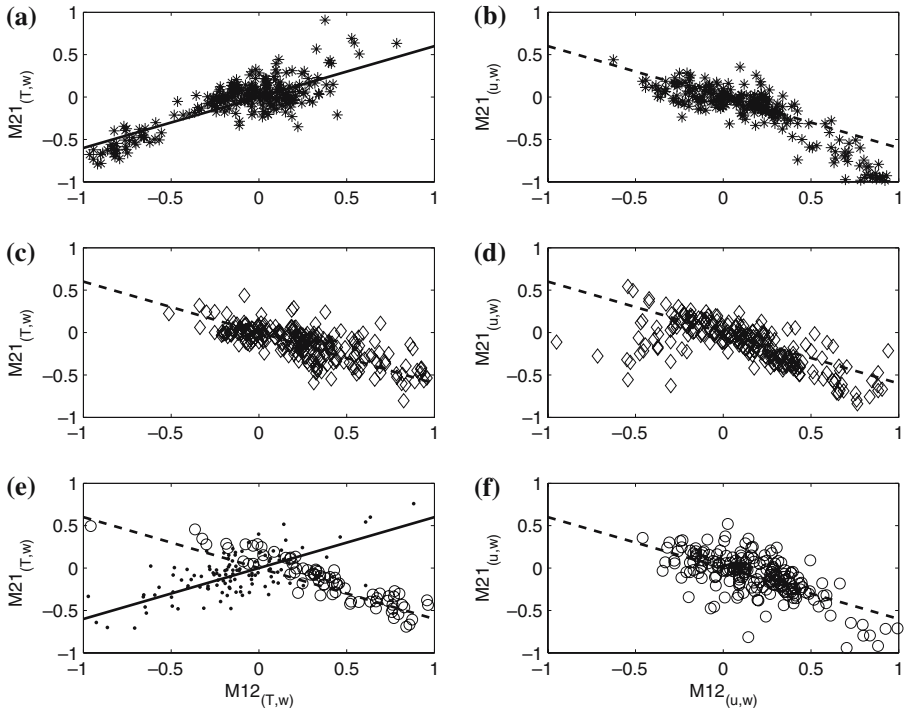

Figure 7. Comparisons between measured M_{12} and M_{21} for momentum and sensible heat for all three stability classes and for all half-hour runs. The three stability classes are: unstable ($*$), weakly stable ($\diamond$), and strongly stable ((o) for the levels where $R_{wT} < 0$ and ($\cdot$) for the levels where $R_{wT} > 0$). The continuous line is $M_{21} = 0.6M_{12}$ and the dashed line is $M_{21} = -0.6M_{12}$. The linear correlation coefficients of the data range between $|R| = 0.70 - 0.88$.

4.4. Relative importance of ejections, sweeps, and atmospheric stability on the sensible heat flux profile

Re-writing Equation (4) as a second-order ODE for the sensible heat flux yields

$$K_t \frac{d^2\overline{w'T'}}{dz} + \frac{dK_t}{dz}\frac{d\overline{w'T'}}{dz} - \frac{C_4}{\tau}\overline{w'T'} = \left[\overline{w'^2}\frac{\partial \overline{T}}{\partial z} - \frac{4}{3}\frac{g}{\overline{T}}\overline{T'^2}\right], \tag{17}$$

where $K_t = C_5\tau\sigma_w^2$. Using measured $\sigma_w(z)$, $\overline{T}(z)$, and $\sigma_T(z)$, and estimating τ from Equation (3), the vertical variation of $\overline{w'T'}(z)$ was computed numerically (see Katul and Albertson, 1999; Siqueira and Katul, 2002 for numerical scheme and details). To investigate the relative importance of ejections and sweeps and atmospheric stability on the profiles of sensible heat flux, three solutions to Equation (17) were analysed. The first retains all the terms in Equation (17) and is hereafter labelled as the "full solution", the second neglects atmospheric stability by setting $\overline{T'^2} = 0$ and is

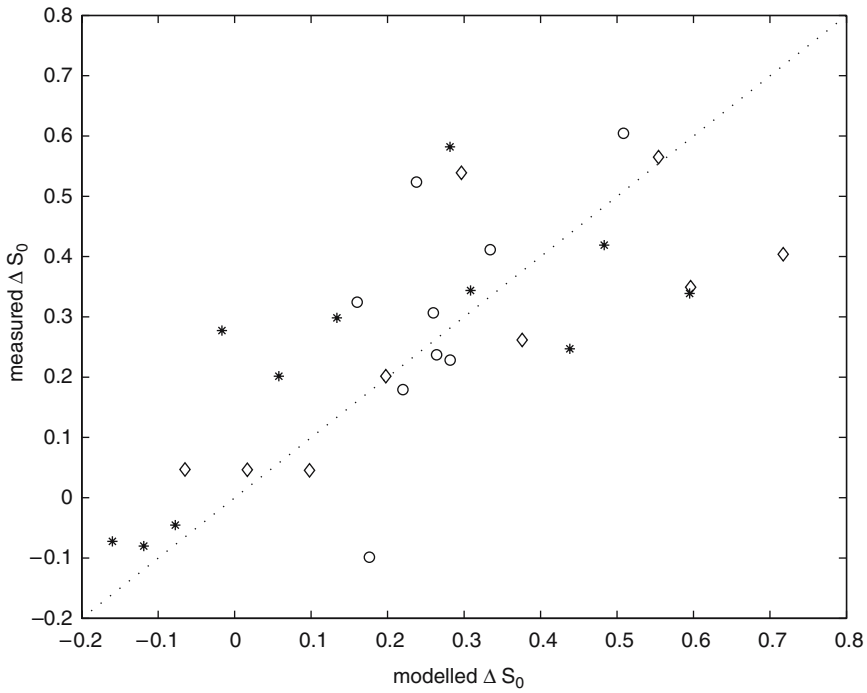

Figure 8. Comparison between measured and modelled ΔS_o for all three stability classes. The modelled ΔS_o is from Equation (16) using the ensemble-averaged measured sensible heat flux and σ_w profiles. The three stability classes are as before: unstable (∗), weakly stable (◇), and strongly stable (o). For reference, the 1:1 line is also shown. The linear correlation coefficient of the data is $R = 0.7$.

labelled the "neutral solution", and the third is a K theory calculation obtained by setting both $\overline{T'^2} = 0$ and $K_t = 0$. The resulting sensible heat flux profiles from these three cases are shown in Figure 9.

It is clear that by accounting for all the terms in Equation (17) (i.e. the full model), the agreement between measured and modelled $\overline{w'T'}$ is superior to predictions made from K theory. In fact, the zero and countergradient flows noted in Section 4.1 are all reasonably reproduced by the full model.

Furthermore, the model intercomparisons suggest that the effect of atmospheric stability on the computed sensible heat flux profiles are comparable to the flux-transport term for unstable and extremely stable conditions. Interestingly, however, accounting for atmospheric stability tended to *worsen* the agreement between measured and modelled sensible heat flux for mildly stable conditions. One possible explanation is that the mildly stable runs included many near-neutral cases (i.e. stability is not important); furthermore, the measured σ_T within canopies is never zero and may be

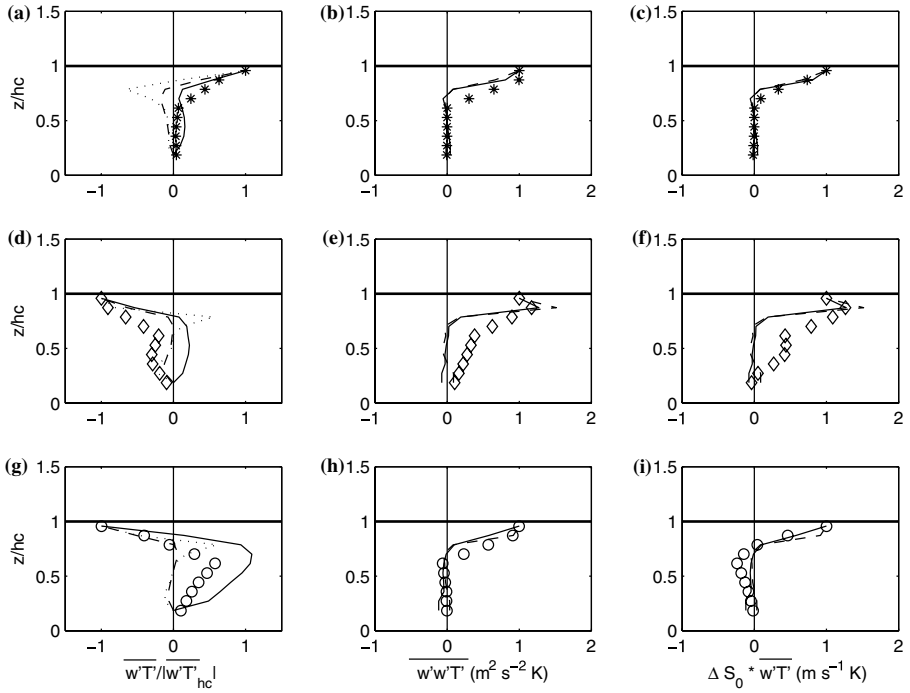

Figure 9. Comparison between measured (symbols) and modelled (line) turbulent statistics within the canopy for, (1) sensible heat flux determined from Equation (17) for unstable (a), weakly stable (d), and strongly stable (g) atmospheric stability; (2) triple velocity-temperature correlations for unstable (b), weakly stable (e), and strongly stable (h) atmospheric stability; (3) $\overline{w'T'}_{\text{sweeps}} - \overline{w'T'}_{\text{ejections}}$ for unstable (c), weakly stable (f), and strongly stable (i) atmospheric stability. For the model comparisons, the solid line is the full model, the dashed line neglects atmospheric stability (neutral model), and the dotted line is the sensible heat flux estimated from K theory.

contaminated by high frequency noise and unsteadiness for this stability class thereby overestimating the computed value of $\frac{4}{3}\frac{g}{\overline{T}}\overline{T'^2}$ from the data. It appears from Figure 9 that neglecting stability for slightly stable flows is even preferred over the full model.

Figure 9 also shows the agreement between measured and modelled $\overline{w'w'T'}$ and $\Delta S_o \times \overline{w'T'} = \overline{w'T'}_{\text{sweeps}} - \overline{w'T'}_{\text{ejections}}$. To our knowledge, testing the skills of second-order closure models using quadrant analysis (i.e. measured $\overline{w'T'}_{\text{sweeps}} - \overline{w'T'}_{\text{ejections}}$) was not conducted before for sensible heat. Again, despite theoretical objections to closing $\overline{w'w'T'}$ via Equation (5) (e.g. Wilson, 1989), the reasonable agreement between measured and modelled $\overline{w'w'T'}$ and $\Delta S_o \times \overline{w'T'}$ for unstable and stable stability classes is rather encouraging. However, the (unexpected) disagreements for slightly stable conditions is rather disappointing.

5. Conclusions

Over the past three decades, experimental and computational developments have led to an extensive understanding of momentum and scalar transfer within uniform canopies. Despite this progress, several unresolved issues remain. The combined effects of buoyancy and ejection-sweep statistics (often signatures of large-scale coherent motion) on scalar transfer is one such issue. To date, no explicit diagnostic model relating the local turbulent heat flux to the mean air temperature gradient, buoyancy, and the statistical properties of the ejection-sweep cycle within the canopy volume exists. To begin progress on this issue, we combined CEM and higher-order closure models and derived explicit linkages between the sensible heat flux, mean temperature profiles, ejection-sweep statistics, and buoyancy. The latter linkages were successfully tested on a dataset collected in a mixed hardwood forest at Lavarone, Italy. Particularly, our analysis and comparisons demonstrated the following:

(1) Second-order closure models for the heat flux budget equation reproduce reasonably well the eddy-covariance measured profiles of $\overline{w'T'}$ and $\overline{w'w'T'}$ for unstable and stable flows. For slightly stable flows, neglecting the buoyancy contribution (i.e. σ_T^2) is preferred (given that σ_T^2 will always be finite inside canopies even for strictly neutral flows).
(2) The CEM and the incomplete CEM (ICEM) proposed by Katul et al. (1997b) are sufficient to link the triple velocity-temperature correlation ($\overline{w'w'T'}$) to ΔS_o. We note that for momentum transfer, Raupach (1981) empirically found a linear relationship between ΔS_o and M_{12} when variations in $u_*^2/(\sigma_u\sigma_w)$ are small (in a wind tunnel). Here, we showed that this linkage depends on the correlation between vertical velocity and scalar concentration.
(3) The ICEM, when combined with the heat flux budget equation, leads to an explicit relationship between $\overline{w'T'}$ and $d\overline{T}/dz$, z, σ_w^2, ΔS_o, and σ_T^2. This relationship must be viewed as diagnostic because the ΔS_o profile is not known *a priori*. Nonetheless, the relationship can be used to estimate $d\overline{T}/dz$ for which zero-gradient (and countergradient) flow occurs if the ejection-sweep cycle properties are *a priori* specified.
(4) Second-order closure models that utilize gradient-diffusion approximation for $\overline{w'w'T'}$, when combined with the ICEM, can estimate ΔS_o. The fact that closure models can estimate ΔS_o offers novel ways of diagnosing closure schemes from quadrant analysis and invites new interpretations to their successes and failures.
(5) The resulting closure model formulation for ΔS_o suggests that sweeps dominate the heat flux when the ratio of the local heat source (S_T) to $\overline{w'T'}$ is positive irrespective of atmospheric stability. Conversely,

ejections dominate the sensible heat flux when $S_T/\overline{w'T'} < 0$. The dominant role of sweeps for unstable and stable atmospheric conditions predicted by the model is consistent with a wide range of field experiments, including the present forest experiment.

From a broader perspective, this study is a necessary first step towards progressing on the general problem of how the ejection-sweep cycle, thermal stratification, dispersive fluxes, and planar inhomogeneous transport (e.g. resulting from topographic or planar canopy density variation) alter flux-gradient relationships at different levels within canopies.

Acknowledgements

Katul and Poggi acknowledge the support of the U.S. National Science Foundation (*NSF-EAR*-02 – 08258), the Biological and Environmental Research (*BER*) Program, U.S. Department of Energy, through the Southeast Regional Center (*SERC*) of the National Institute for Global Environmental Change (*NIGEC*), and through the Terrestrial Carbon Processes Program (*TCP*) and the *FACE* project. Giostra acknowledges the Italian MURST Project "Sviluppo di tecnologie innovative e di processi biotecnologici in condizioni controllate nel settore delle colture vegetali: Diagnosi e Prognosi di situazioni di stress idrico per la vegetazione". Cava acknowledges the CNR for the SHORT-TERM MOBILITY Programme – 2004, and the support of the CNR-ISAC for the Project 'Effetti delle Strutture Coerenti sul Trasporto Turbolento in Canopy Vegetale' (Progetto Giovani Ricercatori CNR-ISAC – 2003). Cescatti acknowledges the support of the Fondazione Cassa di Risparmio di Trento e Rovereto for the Project 'Carbon fluxes and pools in forest ecosystems' and the Province of Trento, Italy, (grant DG 14616/97, DG 1060/01). The authors thank J. Finnigan for his comments on the manuscript.

References

Andre, J. C., de Moor, G., Lacarrere, P., Therry, G., and du Vachat, R.: 1979, 'The Clipping Approximation and Inhomogeneous Turbulence Simulations', *Turbulent Shear Flow*, **I**, 307–318.

Chen, J. M. and Black, T. A.: 1992, 'Defining Leaf-Area Index for Non-flat Leaves', *Plant Cell Environ.* **15**(4), 421–429.

Corrsin, S.: 1974, 'Limitations of Gradient Transport Models In Random Walks and in Turbulence', *Adv. Geophys.* **18**A, 25–60.

Denmead, O. T. and Bradley, E. F.: 1985, 'Flux-Gradient Relationship in a Forest Canopy', in B. A. Hutchinson and B. B. Hicks, (eds), *The Forest Atmosphere Interaction*, D. Reidel Publ. Co. Dordrecht, pp. 421–442.

Fer, I., McPhee, M. G., and Sirevaag, A: 2004, 'Conditional Statistics of the Reynolds Stress in the Under-Ice Boundary Layer', *Geophys. Res. Lett.*, **31**, L15311–L15311.

Finnigan, J. J.: 2000, 'Turbulence in Plant Canopies', *Ann. Rev. Fluid Mech.* **32**, 519–571.

Finnigan, J. J.: 1985, 'Turbulent Transport in Plant Canopies', in B. A. Hutchinson and B. B. Hocks (eds), *The Forest-Atmosphere Interactions*, D. Reidel, Norwell, MA, pp. 443–480.

Finnigan, J. J.: 1979, 'Turbulence in Waving Wheat. II. Structure of Momentum Transfer', *Boundary-Layer Meteorol.*, **16**, 213–236.

Gao, W. G., Shaw, R. H., and Paw U, K. T.: 1989, 'Observation of Organised Structure in Turbulent-Flow Within and Above a Forest Canopy', *Boundary-Layer Meteorol.* **47**, 349–377.

Kaimal, J. C. and Finnigan, J. J.: 1994, *Atmospheric Boundary Layer Flows: Their Structure and Measurements*, Oxford University Press, New York, 289 pp.

Katul, G. G., Cava, D., Poggi, D., Albertson, J. D., and Mahrt, L.: 2004, 'Stationarity, Homogeneity, and Ergodicity in Canopy Turbulence', *Handbook of Micrometeorology*, Chapter 8, Kluwer Academic Publishers, Dordrecht, pp. 84–102.

Katul, G. G., Leuning, R., Kim, J., Denmead, O. T., Miyata, A., and Harazono, Y.: 2001, 'Estimating CO_2 Source/Sink Distributions Within a Rice Canopy Using Higher-Order Closure Models', *Boundary-Layer Metereol.* **98**, 103–125.

Katul, G. G. and Albertson J. D.: 1999, 'Modelling CO_2 Sources, Sinks and Fluxes Within a Forest Canopy', *J. Geophys. Res.* **104**, 6081–6091.

Katul, G. G., Oren, R., Ellsworth, D., Hsieh, C. I., Phillips, N., and Lewin, K.: 1997a, 'A Lagrangian Dispersion Model for Predicting CO_2 Sources, Sinks, and Fluxes in a Uniform Loblolly Pine (Pinus taeda L.) Stand', *J. Geophys. Res.* **102**, 9309–9321.

Katul, G. G., Hsieh, C. I., Kuhn, G., and Ellswort, D.: 1997b, 'Turbulent Eddy Motion at the Forest-atmosphere Interface', *J. Geophys. Res.* **102-D12**, 13409–13421.

Katul, G. G. and Parlange, M. B.: 1994, 'On the Active Role of Temperature in Surface Layer Turbulence', *J. Atmos. Sci.* **51**, 2181–2195.

Leclerc, M. Y., Beissner, K. C., Shaw, R. H., Denhartog, G., and Neumann, H. H.: 1991, 'The Influence of Buoyancy on 3rd-order Turbulent Velocity Statistics Within a Deciduous Forest', *Boundary-Layer Meteorol.* **55**, 109–123.

Leclerc, M. Y., Beissner, K. C., Shaw, R. H., Denhartog, G., and Neumann, H. H.: 1990, 'The Influence of Atmospheric Stability on the Budgets of the Reynolds Stress and Turbulent Kinetic-Energy Within and Above a Deciduous Forest', *J. Appl. Meteorol.* **29**(9), 916–933.

Leuning, R., Denmead, O. T., Miyata, A., and Kim, J.: 2000, 'Source/sink Distributions of Heat, Water Vapour, Carbon Dioxide and Methane in a Rice Canopy Estimated Using Lagrangian Dispersion Analysis', *Agric. For. Meteorol.* **104**, 233–249.

Maitani, T. and Seo, T.: 1985, 'Estimates of Velocity–Pressure and Velocity–Pressure-Gradient Interactions in the Surface Layer Over Plant Canopies', *Boundary-Layer Meteorol.* **33**, 51–60.

Marcolla, B., Pitacco, A., and Cescatti, A.: 2003, 'Canopy Architecture and Turbulence Structure in a Coniferous Forest', *Boundary-Layer Meteorol.* **108**(1), 39–59.

Massman, W. J. and Weil, J. C.: 1999, 'An Analytical One-dimensional Second-Order Closure Model of Turbulence Statistics and the Lagrangian Time Scale Within and Above Plant Canopies of Arbitrary Structure', *Boundary-Layer Meteorol.* **91**(1), 81–107.

Mahrt, L.: 1998, 'Stratified Atmospheric Boundary Layers and Breakdown of Models', *Theoret. Comput. Fluid Dyn.*, **11**, 263–279.

Meyers, T. and Paw U, K. T.: 1987, 'Modelling the Plant Canopy Micrometeorology with Higher-order Closure Principles', *Agric. For. Meteorol.*, **41**, 143–163.

Nagano, Y. and Tagawa, M.: 1995, 'Coherent Motions and Heat Transfer in a Wall Turbulent Shear Flow', *J. Fluid Mech.*, **305**, 127–157.

Nakagawa, H. and Nezu, I.: 1977, 'Prediction of the Contributions to the Reynolds Stress from Bursting Events in Open Channel Flows', *J. Fluid Mech.* **80**, 99–128.

Poggi, D., Katul, G. G., and Albertson, J. D.: 2004, 'Momentum Transfer and Turbulent Kinetic Energy Budgets Within a Dense Model Canopy', *Boundary-Layer Meteorol.* **111**(3), 589–614.

Poggi, D., Albertson J., and Katul, G.: 2005, 'Scalar Dispersion Within a Model Canopy: Measurements and Lagrangian Models', *Adv. Water Res.*, *in press*.

Raupach, M. R.: 1989a, 'Applying Lagrangian Fluid Mechanics to Infer Scalar Source Distributions from Concentration Profiles in Plant Canopies', *Agric. For. Meteorol.* **47**, 85–108.

Raupach, M. R.: 1989b, 'A Practical Lagrangian Method for Relating Scalar Concentrations to Source Distributions in Vegetation Canopies', *Quart. J. Roy. Meteorol. Soc.* **487**, 609–632.

Raupach, M. R.: 1988, 'Canopy Transport Processes', in W. L. Steffen and O. T. Denmead (eds), *Flow and Transport in the Natural Environment*, Springer-Verlag, New York, pp. 95–127.

Raupach, M. R.: 1987, 'A Lagrangian Analysis of Scalar Transfer in Vegetation Canopies', *Ann. Rev. Fluid. Mech.* **13**, 97–129.

Raupach, M. R., Coppin, P. A., and Legg, B. J.: 1986, 'Experiments on Scalar Dispersion Within a Model-Plant Canopy. 1. The Turbulence Structure', *Boundary-Layer Meteorol.* **35**, 21–52.

Raupach, M. R.: 1983, 'Near-Field Dispersion from Instantaneous Sources in the Surface-Layer', *Boundary-Layer Meteorol.*, **27**, 105–113.

Raupach, M. R., Shaw, R. H.: 1982, 'Averaging Procedures for Flow Within Vegetation Canopies', *Boundary-Layer Meteorol.*, **22**, 79–90.

Raupach, M. R.: 1981, 'Conditional Statistics of Reynolds Stress in Rough-wall and Smooth-Wall Turbulent Boundary Layers', *J. Fluid Mech.*, **108**, 363–382.

Shaw, R. H.: 1977, 'Secondary Wind Speed Maxima Inside Plant Canopies', *J. Appl. Meteorol.* **16**(5), 514–521.

Shaw, R. H., Gao, W. G., and Paw U, K. T.: 1989, 'Detection of Temperature Ramps and Flow Structures at a Deciduous Forest Site', *Agric. For. Meteorol.* **47**, 123–138.

Siqueira, M., Leuning, R., Kolle, O., Kelliher, F. M., and Katul, G. G.: 2003, 'Modeling Sources and Sinks of CO_2, H_2O and Heat Within a Siberian Pine Forest Using three Inverse Methods', *Quart. J. Roy. Meteorol. Soc.* **129**, 1373–1393.

Siqueira, M., Katul, G. G., and Lai, C. T.: 2002, 'Quantifying Net Ecosystem Exchange by Multilevel Ecophysiological and Turbulent Transport Models', *Adv. Water Res.*, **25**, 1357–1366.

Siqueira, M. and Katul, G. G.: 2002, 'Estimating Heat Sources and Fluxes in Thermally Stratified Canopy Flows Using Higher-order Closure Models', *Boundary-Layer Meteorol.* **103**, 125–142.

Thurtell., G. W.: 1989, 'Comment on Using K-theory Within and Above the Plant Canopy to Model Diffusion Processes', in *Estimation of Areal Evapotranspiration*, IAHS plubl., Vol. **177**, pp. 43–80.

Valentini, R., Matteucci, G., Dolman, A. J., Schulze, E. D., Rebmann, C., Moors, E. J., Granier, A., Gross, P., Jensen, N. O., Pilegaard, K., Lindroth, A., Grelle, A., Bernhofer, C., Grunwald, T., Aubinet, M., Ceulemans, R., Kowalski, A. S., Vesala, T., Rannik, U., Berbigier, P., Loustau, D., Guomundsson, J., Thorgeirsson, H., Ibrom, A., Morgenstern, K., Clement, R., Moncrieff, J., Montagnani, L., Minerbi, S., and Jarvis, P. G.: 2000, 'Respiration as the Main Determinant of Carbon Balance in European Forests', *Nature*, **404**, 861–865.

Wilson, N. R.: 1989, 'Turbulent Transport Within the Plant Canopy', in *Estimation of Areal Evapotranspiration*, IAHS publ., Vol. **177**, pp. 43–80.

Wilson, N. R. and Shaw, R. H.: 1977, 'A Higher Order Closure Model for Canopy Flow', *J. Appl. Meteorol.* **16**, 1197–1205.

Wyngaard, J. C.: 1982, *Boundary-layer Modelling, in Atmospheric Turbulence and Air Pollution Modelling*, F. T. M. Nieuwstadt and H. van Dop (eds), D. Reidel, Dordrecht, pp. 69–158.